

See discussions, stats, and author profiles for this publication at: <https://www.researchgate.net/publication/282875990>

Stability of Catalyzed Magnesium Hydride Nano-Crystalline During Hydrogen Cycling. Part I: Kinetic Analysis

ARTICLE in THE JOURNAL OF PHYSICAL CHEMISTRY C · OCTOBER 2015

Impact Factor: 4.77 · DOI: 10.1021/acs.jpcc.5b06190

CITATION

1

READS

78

3 AUTHORS:



[Chengshang Zhou](#)

University of Utah

14 PUBLICATIONS 161 CITATIONS

[SEE PROFILE](#)



[Zhigang Zak Fang](#)

University of Utah

156 PUBLICATIONS 2,186 CITATIONS

[SEE PROFILE](#)



[Robert Bowman](#)

Oak Ridge National Laboratory

275 PUBLICATIONS 3,837 CITATIONS

[SEE PROFILE](#)

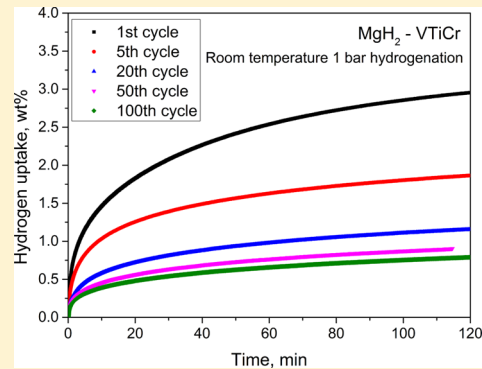
Stability of Catalyzed Magnesium Hydride Nanocrystalline During Hydrogen Cycling. Part I: Kinetic Analysis

Chengshang Zhou, Zhigang Zak Fang*, and Robert C. Bowman, Jr.

Department of Metallurgical Engineering, The University of Utah, 135 South 1460 East, Room 412, Salt Lake City, Utah 84112-0114, United States

S Supporting Information

ABSTRACT: Magnesium hydride is widely recognized as a promising material for hydrogen storage and thermal energy storage. Cyclic stability of the kinetics of catalyzed MgH_2 was systematically investigated in this study. Three systems including $\text{MgH}_2\text{-TiH}_2$, $\text{MgH}_2\text{-TiMn}_2$, and $\text{MgH}_2\text{-VTiCr}$ were prepared by high energy ball milling. Volumetric hydrogen desorption and absorption cycles were performed using the pressure–composition–isothermal (PCI) method. Results show that the kinetics of high-temperature (300°C) hydrogenation and dehydrogenation maintained a good stability during 100 hydrogen cycles. However, when testing the hydrogenation kinetics at the low-temperature range from 25 to 150°C , a severe degradation was observed after hydrogen cycles. Among the three materials, the $\text{MgH}_2\text{-VTiCr}$ system shows better cyclic performance. The degradation of low-temperature kinetics can be mainly related to the hydrogenation–dehydrogenation cycling reactions.



1. INTRODUCTION

Magnesium hydride (MgH_2) is considered as a promising candidate for both hydrogen storage material^{1–4} and thermal energy storage^{5–7} due to its high theoretical hydrogen capacity (7.6 wt %), good reversibility, low cost, and high energy density—namely, a high enthalpy (75 kJ/mol H₂) of endothermic and exothermic reactions of magnesium and hydrogen.^{8–12} However, the conditions of temperature and pressure for the dehydrogenation and rehydrogenation cycles of MgH_2 are generally rather stringent to achieve adequate kinetic rates. For example, a temperature above 300°C is needed for the reverse cycling (dehydrogenation and hydrogenation reactions). The hydrogenation often requires hydrogen pressure higher than 10 bar, and the dehydrogenation takes place under vacuum.

In the past decades, tremendous efforts have been directed to improve the kinetics of MgH_2 . Now a general consensus is that the kinetics rate can be boosted by (1) reducing Mg/ MgH_2 to nanoscale using various techniques such as mechanical milling^{13–17} and thin-film deposition^{18–21} and (2) doping with transition metal and transition metal compound such as Ti,¹³ V,^{13,22} Nb,^{22,23} and Nb_2O_5 .^{24–26} In particular, recent research showed that some transition metal compounds provided strong catalytic effects that can enhance the kinetics significantly. For example, Lu et al.^{27,28} showed that TiH_2 catalyzing contributed to a significant improvement of dehydrogenation and hydrogenation reactions compared to undoped MgH_2 . Zahiri et al. reported a number of bimetal catalysts including Cr–V,²⁹ Cr–Ti,³⁰ Fe–V,³¹ and Fe–Ti³² that lead to hydrogen uptake of Mg at moderate temperature. Furthermore, our recent studies^{33–36} reported that doping with

the TiMn_2 or VTiCr catalysts leads to hydrogenation of Mg at room temperature and 1 bar pressure.

When the kinetics of MgH_2 have been improved, an important characteristic for the practical use of MgH_2 is its cycle life.³⁷ Dehouche et al.³⁸ investigated the effect of long-term cycling on the hydrogenation and dehydrogenation properties of the $\text{MgH}_2\text{-V}$ nanocomposite. Their result exhibited an overall good reversibility and only a slight deterioration in desorption rate at 300°C after 2000 cycles. The group of Mitlin reported hydrogen cycling tests for Mg–Cr–V,²⁹ Mg–Nb–V,³⁹ Mg–Fe–Ti,^{19,32,40,41} Mg–Al–Ti,^{41,42} and Mg–Cr–Ti³⁰ nanocomposites which had been synthesized by the physical vapor deposition (PVD) method. In particular, their study on binary Mg–Nb and ternary Mg–V–Nb systems³⁹ suggested that the microstructure of the hydride materials changed significantly due to hydrogen cycles for 500 times. Given the fact that the Mg/ MgH_2 grain tends to coarsen and agglomeration of the catalyst may occur during the hydrogenation and dehydrogenation cycling, a rational concern will be the long-term stability of Mg/ MgH_2 and catalyst nanocrystallines. Moreover, practical cycling of a hydride system is likely to be at a complicated condition such as varying temperature and low-pressure hydrogen supply. The reported literature, however, focused on the cycling performance of Mg-based hydride under such conditions is limited. Therefore, a comprehensive study is desired to evaluate the

Received: June 28, 2015

Revised: August 3, 2015

Published: September 11, 2015



cycling behavior of the kinetics at low temperature and under low hydrogen pressure differentiation (low driving force).

In this paper, a comprehensive investigation is designed to study the kinetic stability of nanocrystalline MgH₂ doped with transition metal catalysts. The doped MgH₂ used in the present work was produced using an ultrahigh-energy–high-pressure (UHEHP) milling technique.³⁶ The first objective is to evaluate the stability of the kinetics of catalyzed MgH₂ during high-temperature hydrogen cycling. The second purpose is to examine room-temperature hydrogenation behaviors after cycling duration using different conditions. Correlated to the kinetics analysis, further characterization on the microstructure is present in Part II of this manuscript (<http://dx.doi.org/10.1021/acs.jpcc.Sb06192>).

2. EXPERIMENTAL SECTION

The raw materials for this work, MgH₂ powder (Sigma-Aldrich, 683043), TiH₂ powder (Sigma-Aldrich, 209279), and TiMn₂ alloy powder (composition: Ti_{0.98}Zr_{0.02}V_{0.43}Fe_{0.09} Cr_{0.05}Mn_{1.5}, Sigma-Aldrich, 685941) were purchased from Sigma-Aldrich (Milwaukee, WI). 75V–5Ti–20Cr alloy (75 mol % vanadium, 5 mol % titanium, and 20 mol % chromium) was custom-made at the Materials Preparation Center of the Ames Laboratory (Ames, IA) by using the arc-melting technique and then was pulverized into powder. Afterward, five grams of mixtures of MgH₂ with additives in 5% molar ratios was milled using a custom-made UHEHP planetary ball milling machine under a 150 bar hydrogen pressure.¹⁴ The ball-to-powder ratio was 10:1 by volume, and the milling was carried out for 4 h at room temperature. All material handling was carried out in a glovebox filled with purified argon (99.999%), with water vapor and oxygen concentrations both at less than 1 ppm.

Volumetric cycling measurements and equilibrium pressure measurements using the pressure–composition–isothermal (PCI) method were performed on an automated Sieverts-type apparatus (Hy-Energy LLC, PCTPro-2000). About 0.1 g of each milled powder was loaded into a stainless steel vessel and sealed in a sample holder. During the experiments, the sample temperatures were held constant by a PID heating controller (Watlow, PID Controller SD). The equilibrium pressure data were collected at 300 °C. The equilibrium point was determined when the reaction rate was less than 1×10^{-5} wt %/min for 1 min. In this work, four different types of tests were performed, as described below.

2.1. Isothermal Cycling. Isothermal cycling tests were conducted to evaluate the dehydrogenation kinetics under a low driving force (low hydrogen pressure differentiation during dehydrogenation). Samples were held under isothermal conditions throughout the cycling. During the isothermal cycling, the temperature of the samples was maintained constantly at 250 and 270 °C. Hydrogenation occurred when 10 bar hydrogen pressure was introduced to the sample. Dehydrogenation occurred after reducing the hydrogen pressure from 10 to 0.2 bar for the 250 °C dehydrogenation and from 10 to 0.5 bar for the 270 °C dehydrogenation. The cycles was performed using the programmable PCT-Pro 2000 Sieverts-type machine.

2.2. Isothermal Cycling with Intermittent Low-Temperature Hydrogenation Evaluation. A set of cycling tests were performed to evaluate the stability of low-temperature hydrogenation after a number of thermal cycles. Samples were cycled under an isothermal temperature (250, 300, and 350 °C). Each step (i.e., repeating the dehydrogenation–

hydrogenation reactions) of cycling was controlled by the PCT-Pro 2000 machine. During the cycling, hydrogenation was performed after introducing 4 bar hydrogen pressure to the sample chamber, and the dehydrogenation was performed after the pressure was reduced from 4 to 0.01 bar. To conduct low-temperature hydrogenation tests, the control program was manually suspended, and the cycling process was interrupted after specified numbers of cycles, namely, at the 1st, 5h, 20th, 50th, and 100th cycle. After the program was stopped, the sample chamber was evacuated by a vacuum pump for 30 min to ensure that the sample was fully dehydrogenated. Then the dehydrogenated samples were cooled to a low temperature (25, 60, 100, or 150 °C) for an isothermal hydrogenation test. After the hydrogenation test, the sample was heated again to the previous cycling temperature (high temperature), and then the isothermal cycling continued.

2.3. Nonisothermal Cycling. Further investigation was performed by applying oscillating temperatures⁴³ (a thermal cycle is varied from 290 to 330 °C) to catalyzed MgH₂. In the experiment, around 100 mg of sample was sealed in a chamber with a volume of 18 mL. The cycling was performed by using the PCT-Pro 2000 machine. During the experiments, the sample temperatures were adjusted by the PID heating controller (Watlow, PID Controller SD). A detailed temperature profile and kinetic curve of the cycling were provided in the Supporting Information. As shown in Figure S1, 100 cycles were carried out, and each cycle included the following steps

- (1) A heating stage (290–330 °C): The sample was heated from 290 to 330 °C in 15 min. During this stage the equilibrium pressure of MgH₂ continuously raised. Due to the equilibrium increase, heating the sample leads to dehydrogenation of the sample.
- (2) A cooling stage (330 to 290 °C): The sample was cooled from 330 to 290 °C in 7 min. During this stage the equilibrium pressure of MgH₂ continuously dropped. Because the equilibrium decreased, the sample absorbed hydrogen from the environment.

2.4. Annealing under Different Conditions. The experiment was designed to evaluate the kinetics of the catalyzed MgH₂ sample after annealing under different pressure and temperature conditions. A dehydrogenation and hydrogenation using the same parameters were performed before and after annealing the catalyzed MgH₂ sample under specified temperature and hydrogen pressure. The annealing time was kept at 40 h. The experimental procedure is described as follows:

- (1) 300 °C dehydrogenation under 0.01 bar pressure.
- (2) Room-temperature hydrogenation under 1 bar pressure.
- (3) Isothermal annealing for 40 h under specified pressure and temperature conditions.
- (4) Recharge the sample at 300 °C with 10 bar H₂, and then a 300 °C dehydrogenation test was performed under 0.01 bar pressure.
- (5) Room-temperature hydrogenation test under 1 bar pressure.

3. RESULTS

3.1. Dehydrogenation Kinetics. It has been reported that a catalyzed MgH₂ system showed good stability when cycling at a temperature of 300 °C.^{38,44} Isothermal cycling experiments were designed for evaluating dehydrogenation kinetics under relatively low temperatures (250 and 270 °C) and low

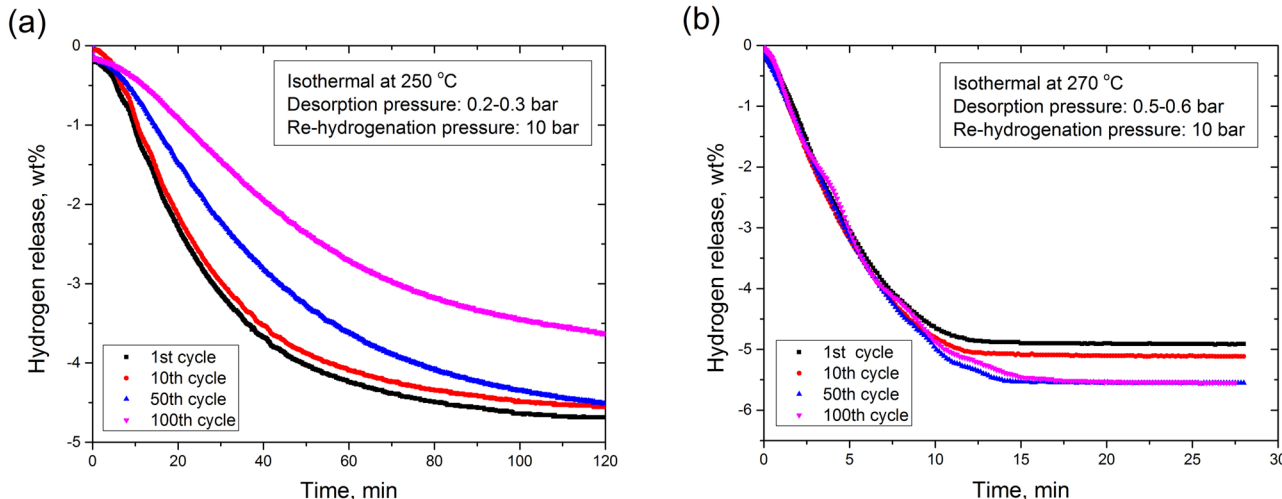


Figure 1. Dehydrogenation kinetics at different cycles. (a) Tests performed at 250 °C. (b) Tests performed at 270 °C.

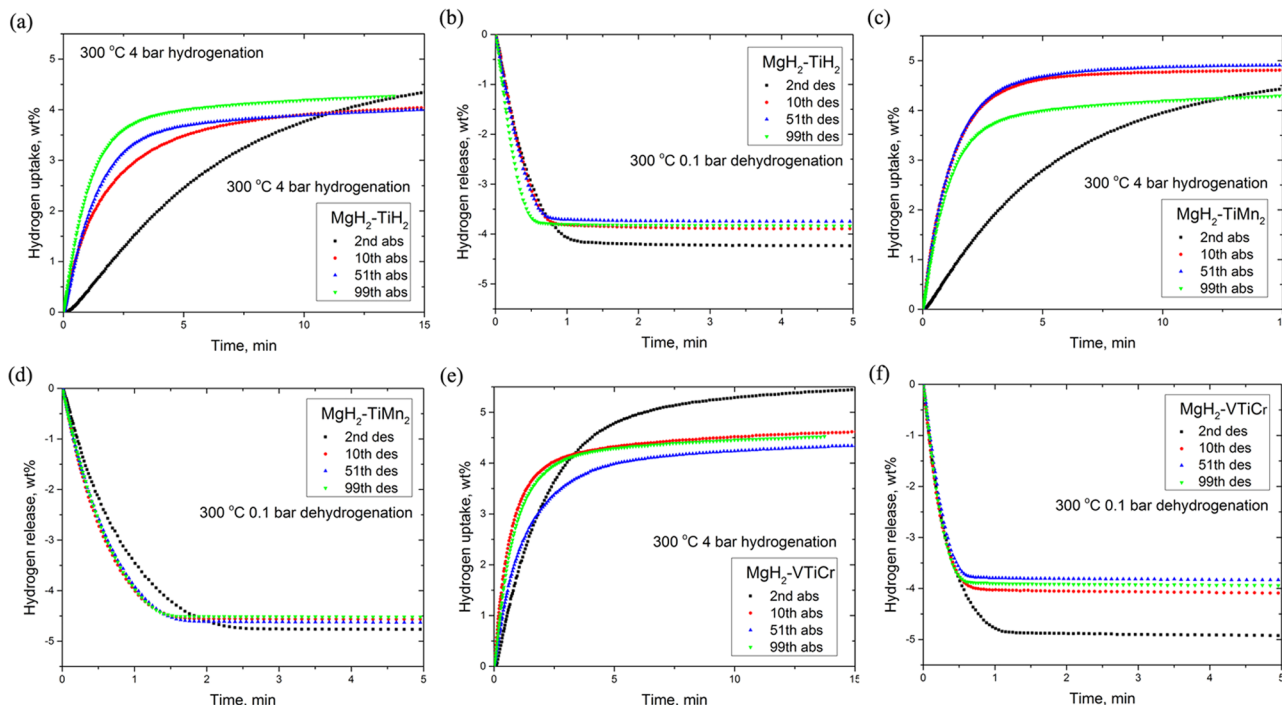


Figure 2. 300 °C hydrogenation and dehydrogenation kinetics at different cycles. (a) Hydrogenation of the MgH₂-TiH₂ system. (b) Dehydrogenation of the MgH₂-TiH₂ system. (c) Hydrogenation of the MgH₂-TiMn₂ system. (d) Dehydrogenation of the MgH₂-TiMn₂ system. (e) Hydrogenation of the MgH₂-VTiCr system. (f) Dehydrogenation of the MgH₂-VTiCr system.

hydrogen pressure differentiation. The MgH₂-VTiCr system was cycled in the present experiments. Figure 1(a) and (b) shows the comparisons of the dehydrogenation kinetics at temperatures of 250 and 270 °C at different cycles (the 1st, 10th, 50th, and 100th). The cyclic experiments were carried out using the procedure described in section 2.1. In order to keep the driving forces of the dehydrogenations low, the dehydrogenations were carried out in a pressure range from 0.2 to 0.3 bar at 250 °C ($P/P_{eq} = 0.54\text{--}0.79$) and in a pressure range from 0.5 to 0.6 bar at 270 °C ($P/P_{eq} = 0.68\text{--}0.82$). Although different pressures were used during the dehydrogenation of the two tests, their hydrogenation reactions used the same hydrogen pressure (10 bar). As shown in Figure 1(a), after 10 cycles at 250 °C, the dehydrogenation kinetics degraded. The desorption rate of the 50th cycle is slightly

slower than those of the 1st and 10th cycles. At the 100th cycle the rate is significantly slower and only released 3.5 wt % of hydrogen in 120 min. On the other hand, when the test temperature was increased to 270 °C (Figure 1(b)), no obvious degradation was observed. Moreover, it is interesting to see that with temperature increasing only 20 °C much faster kinetics can be achieved. For the dehydrogenation performed at 270 °C, approximately 5 wt % hydrogen was desorbed in less than 15 min, compared to the release of 3.5–4.5 wt % hydrogen in 120 min at 250 °C.

3.2. Effect of Different Catalysts on the Kinetics. The cyclic experiments for the 5 mol % TiH₂-catalyzed, 5 mol % TiMn₂-catalyzed, and 5 mol % VTiCr-catalyzed MgH₂ systems were conducted following the procedure described in section 2.2. The cycling temperature was 300 °C. The hydrogenation

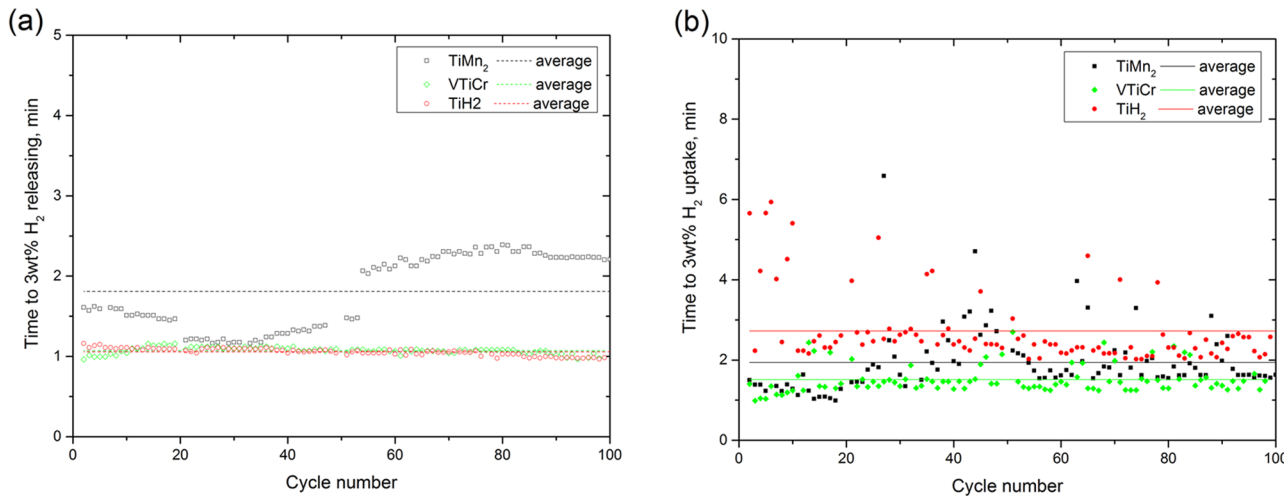


Figure 3. Plot of time-to-3 wt % hydrogen release and uptake as a function of cycle number. The samples were cycled at 300 °C. (a) Hydrogen release. (b) Hydrogen uptake.

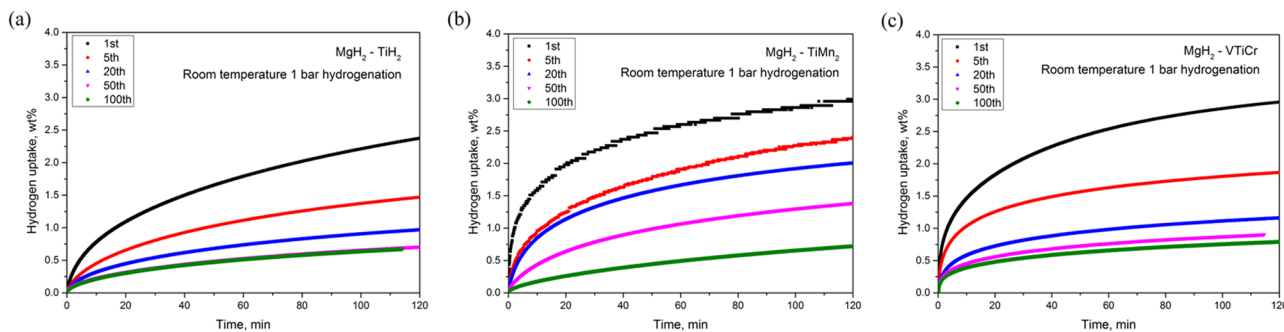


Figure 4. Room-temperature hydrogenation kinetics after different cycles of MgH₂-TiH₂, MgH₂-TiMn₂, and MgH₂-VTiCr, the isothermal cycling tests performed at 300 °C. (a) MgH₂-TiH₂; (b) MgH₂-TiMn₂; (c) MgH₂-VTiCr.

and dehydrogenation kinetics during the thermal cycling were compared in Figure 2, showing the kinetics at different cycles (the 2nd, 10th, 51st, and 99th) for both hydrogenation kinetics and dehydrogenation kinetics of the three systems. It can be seen that the three materials present sluggish kinetics in the initial stage of cycling (2nd cycle) compared to the kinetics of later cycles (10th, 51st, and 99th cycles). For the hydrogenation rate, it slightly improved and became stable as the cycle was progressed. However, the dehydrogenation kinetic rates at different cycles were almost unchanged compared to those of the hydrogenation. There are losses of hydrogen storage capacity after the cycling for all the systems. The hydrogen capacities of different samples reduced 0.4 wt % for TiH₂-catalyzed MgH₂, 0.2 wt % for TiMn₂-catalyzed MgH₂, and 1.0 wt % for VTiCr-catalyzed MgH₂. Similar to the evolution of kinetics, the reduction of the capacities generally occurred in the first 10 cycles.

Further analysis was conducted to compare the three systems in detail through plotting the values of time-to-3 wt % hydrogen uptake/release against the cycle number, as shown in Figure 3. The figure provides a panoramic evolution of the kinetics during the 100 cycles. First, no obvious kinetic degradation for both desorption and absorption of all the systems is observed. Second, comparing the variances of the kinetics from the three hydride systems, the dehydrogenation kinetics seem to be more stable than those of hydrogenation, or in other words, the hydrogenation rates are more scattered through the cycling compared to dehydrogenation. The

variances of kinetics at different cycles are probably due to the deviation of hydrogen pressure provided by the PCT machine when the cycling was performed. Third, according to the average of the kinetic rates from the 100 cycles, the MgH₂-TiH₂ and MgH₂-VTiCr present better desorption kinetics, and the MgH₂-VTiCr had the best absorption kinetics. Among the three different systems, the MgH₂-VTiCr material seems to be more robust against the thermal cycling regarding its kinetic rates of both hydrogenation and dehydrogenation.

Previous studies^{28,34} demonstrated that catalyzed Mg nanoparticles were capable of absorbing a significant amount of hydrogen at room temperature. However, reported research on the stability of the room-temperature hydrogenation kinetics after hydrogen cycles is very limited. To examine this, the cycling tests of MgH₂-TiH₂, MgH₂-TiMn₂, and MgH₂-VTiCr samples were interrupted when the cycling had completed the 1, 5, 20, 50, and 100 cycles. During the intermissions, the samples were cooled to room temperature, and a hydrogenation test was performed under 1 bar hydrogen pressure. The results of hydrogenation kinetic curves were compared in Figure 4, showing an obvious degradation for all the catalyzed materials. Take the MgH₂-VTiCr system for example: a hydrogen uptake of 3.0 wt % in 120 min was observed after the first cycle. However, after 100 cycles, only 1.0 wt % of hydrogen was absorbed over the same period of time. Among the three systems, MgH₂-VTiCr exhibits relatively the best hydrogenation properties against the cyclic degradation.

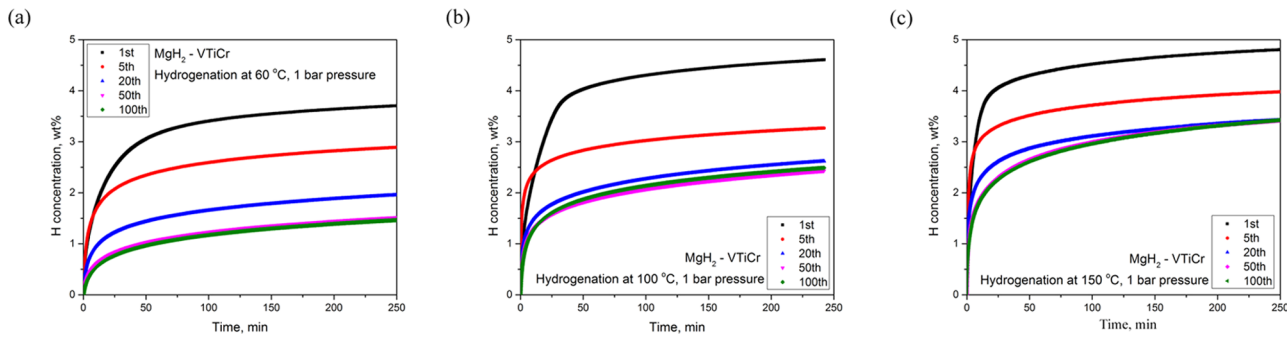


Figure 5. Hydrogenation kinetics at different temperature after different cycles of $\text{MgH}_2\text{-VTiCr}$, where the isothermal cycling was performed at 300 °C. (a) Hydrogenation tests were performed at 60 °C. (b) Hydrogenation tests were performed at 100 °C. (c) Hydrogenation tests were performed at 150 °C.

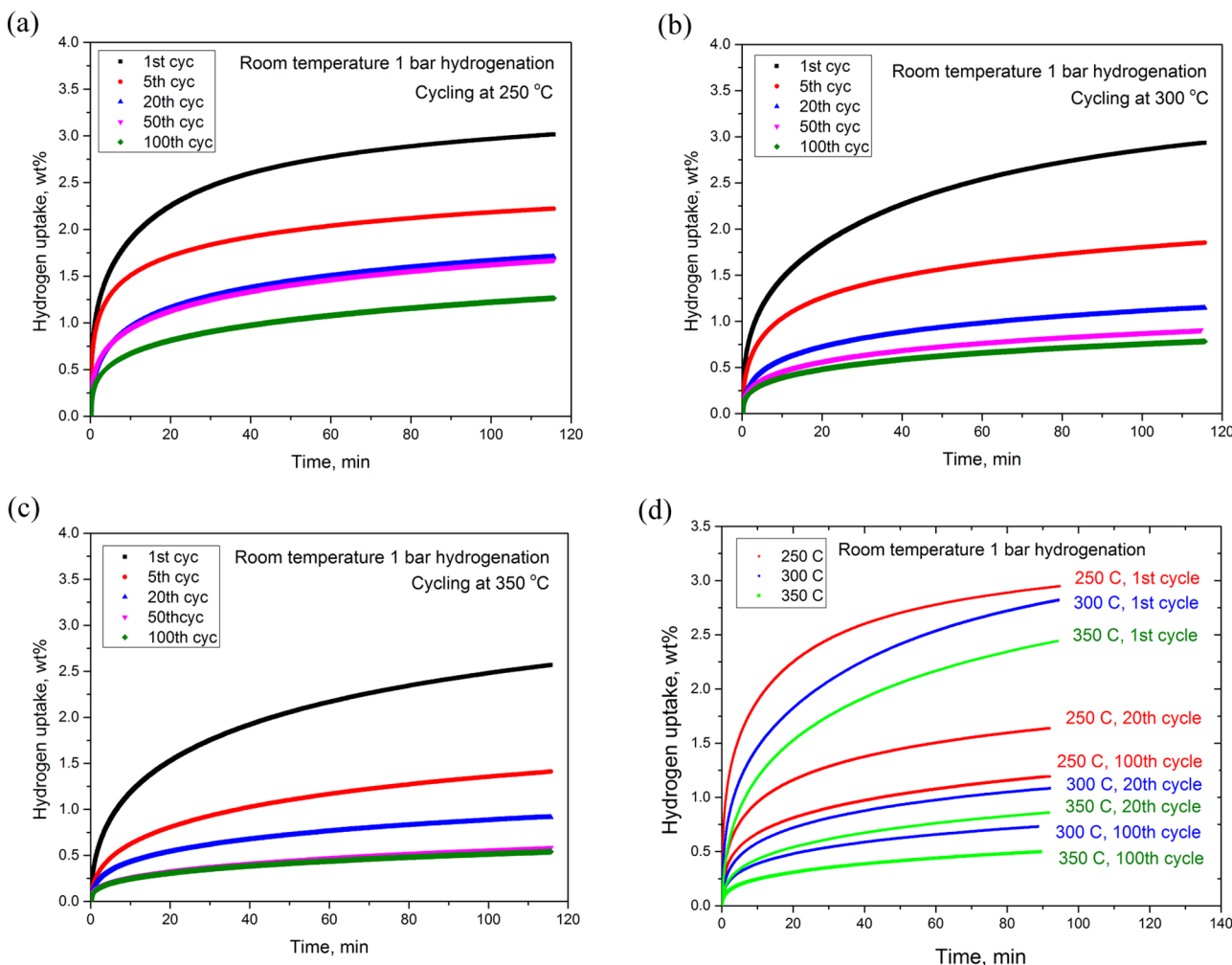


Figure 6. Effect of cycling temperature on room temperature (1 bar) hydrogenation rates of $\text{MgH}_2\text{-VTiCr}$. (a) The isothermal cycling tests performed at 250 °C. (b) Tests performed at 300 °C. (c) Tests performed at 350 °C. (d) Comparison of kinetics at different temperatures.

3.3. Low-Temperature Hydrogenation Kinetics under Different Temperature Conditions. The above results demonstrated severe degradations of the room-temperature hydrogenation kinetics of the catalyzed MgH_2 samples after extended hydrogen cycling. However, it is also shown that the kinetics at high temperature, namely, at 300 °C, did not deteriorate during the cycling. To find out the temperature dependence of hydrogenation kinetics on the degradation behavior, three experiments were conducted using the same

material and the same procedure described above (section 2.2). Instead of measuring the kinetics at room temperature, different temperatures (60, 100, and 150 °C) were applied to perform the 1 bar hydrogenation tests.

Figure 5 shows the comparisons of the degradation behavior of the hydrogenation kinetics at 60, 100, and 150 °C. It can be seen that the degradation still took place in the course of 1–50 cycles for the 60 °C hydrogenation tests and in the course of 1–20 cycles for the 100 °C hydrogenation tests. Results also

showed that when the cycling was further extended the degradation rate tended to diminish. For example, the 60 °C kinetics after 50 cycles showed no significant degradation; the 100 °C hydrogenation after 20 cycles showed no obvious decrease as well. When the hydrogenation temperature was further increased to 150 °C, the degradation of the kinetics was still observed in the first 20 cycles, which is similar to the tests at 100 °C. In addition, the kinetics after 100 cycles shows 3.3 wt % hydrogen uptake in 250 min, which is higher than the room-temperature hydrogen absorption after 1 cycle.

3.4. Effect of Cycling Temperature on Room-Temperature Hydrogenation. The effect of cycling temperature (250, 300, and 350 °C) on room-temperature hydrogenation kinetics was studied, and the kinetics (after 1, 5, 20, 50, and 100 cycles) were shown in Figure 6. The MgH₂–VTiCr system was used for the cycling measurement. The effect of cycling temperatures on the degradation behavior of the room-temperature hydrogenation kinetics (after 1, 20, and 100 cycles) was given in Figure 6(d), showing that the cycling temperature has a significant impact on the performance of subsequent room-temperature hydrogenation—higher cycling temperature results in faster rate of degradation. The thermally induced impact on the degradation behavior is so significant that the differences of the kinetic appeared even after the first cycle at the different temperatures of 250, 300, and 350 °C.

3.5. Effect of Packing Status of the Material on Room-Temperature Hydrogenation. Two MgH₂–VTiCr samples with different packing densities were prepared and tested. The cycling experiments were followed by the procedure described in experimental section 2.2, and the hydrogenation tests were performed at 25 °C. One sample was loose powder with density in a range of 0.45 g/cm³ and estimated porosity of 71 vol %. Another sample used the same batch of material but was pressed into a dense pellet with a density of 1.06 g/cm³ and a porosity of 31.6 vol %, as listed in Table 1. The two samples

Table 1. Sample Density and Porosity of the Loose Powder and Compact Pellet

samples	density, g/cm ³	porosity, %	mass of dose, g
loose MgH ₂ –VTiCr powder	0.45	71	0.1861
compact MgH ₂ –VTiCr pellet	1.06	31.6	0.1712

were then loaded into vessels for comparative tests. As shown in Figure 7, the two samples exhibited the similar kinetics and degradation rate, indicating that the packing status of catalyzed MgH₂ in terms of the density and porosity of the material has no influence on not only the hydrogenation kinetics but also the degradation behavior.

3.6. Effect of Annealing under Different Conditions. The present assessments on room-temperature hydrogenation kinetics show that deterioration gradually occurred with extending cycling. It is recognized that during the above variable-pressure cycling tests the phase compositions of the samples were kept changing during the repeating hydrogenation and dehydrogenation reactions. To simplify the problem, a set of experiments were designed to evaluate the effect of annealing the sample at different isothermal and constant pressure conditions for a period of time (40 h). Therefore, the phase compositions during the course of annealing would not vary. These experiments examined kinetic difference of the material before and after annealing.

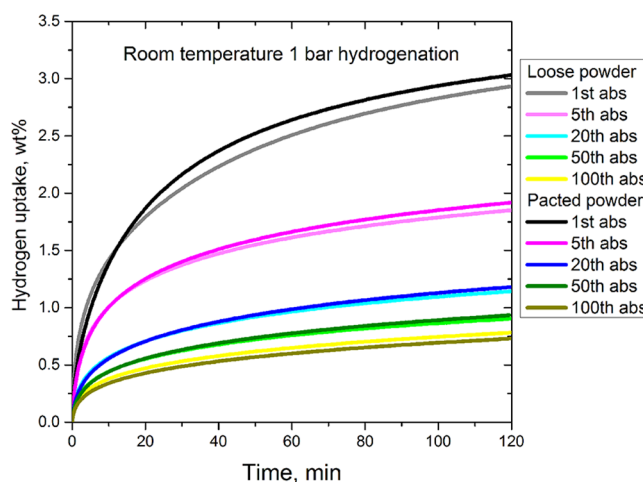


Figure 7. Room-temperature hydrogenation kinetics of packed and unpacked powder samples after different cycles.

The temperature and pressure conditions for annealing were described in Table 2. Before and after annealing, dehydrogen-

Table 2. Temperature and Hydrogen Pressure Conditions for Annealing

test number	temperature, °C	pressure, bar	phase (Mg or MgH ₂)
1	300	10	MgH ₂
2	300	1	Mg
3	300	0 (sample sealed in closed vessel)	Mg
4	300	0 (sample was actively vacuum pumped)	Mg
5	25	0 (sample was actively vacuum pumped)	Mg

ation and hydrogenation tests were performed, and the detailed procedure given in experimental section 2.4 was followed. The comparisons of the kinetics curves are plotted in Figure 8. From Figure 8(a) and (b), it can be seen that there is essentially no degradation after the sample was annealed at pressurized hydrogen (10 bar) and 300 °C (test No. 1). Both the hydrogenation and dehydrogenation kinetics slightly improved after the annealing. The improvement of kinetics is probably attributed to removal of contaminant(s) on the surface of the material.

In the tests No. 2 and No. 3, the samples were annealed at the same temperature (300 °C), but the pressures were reduced to 1 and 0 bar, respectively. Consequently, the primary phase of the material during the annealing will be Mg metal under those pressures. As shown in Figure 8(c) and (e), moderate degradation was shown on both room-temperature hydrogenation and 300 °C dehydrogenation kinetics after the annealing. The curves of dehydrogenation after the annealing also showed incubation phenomena, where the materials did not start to desorb hydrogen in the beginning but incubated for a period of time (~10 min in these cases). Despite this behavior, it is recognized from No. 2 and No. 3 tests that high-temperature annealing for the dehydrogenated sample (Mg) has only limited impact on the kinetic rates.

The sample in test No. 4 was continuously evacuated by a vacuum pump (ultimate pressure 1.6×10^{-2} mbar) while being heated to 300 °C for 40 h. In comparison to test No. 3, the

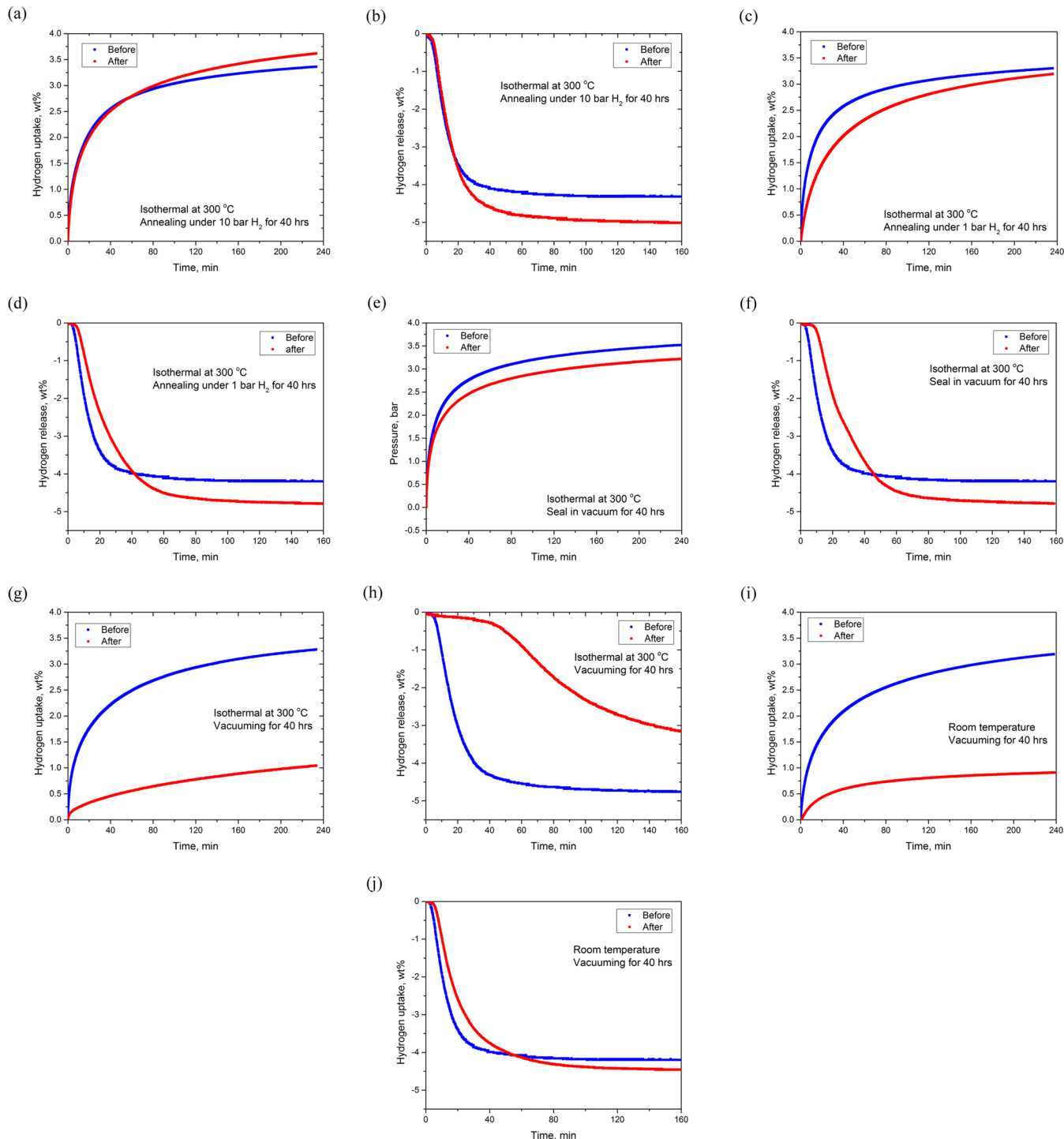


Figure 8. Comparisons of hydrogenation kinetics and dehydrogenation kinetics of MgH₂–VTiCr before (blue) and after (red) different annealing conditions: (a) and (b) 300 °C and 10 bar hydrogen pressure; (c) and (d) 300 °C and 1 bar hydrogen pressure; (e) and (f) 300 °C and 0 bar hydrogen pressure; (g) and (h) 300 °C and vacuuming; (i) and (j) 25 °C and vacuuming. All the annealing times were 40 h.

annealing temperature and pressure of test No. 4 were kept approximately the same as in No.3. However, the hydrogenation and dehydrogenation became significantly sluggish, as shown in Figure 8(g) and (h). This rules out the possibility that the degradation was due to the decomposition of VTiCr or diffusions of catalytic elements under such a condition. Therefore, contamination and/or oxidization (O₂ and H₂O) to the sample likely occurred due to the long-term vacuum pumping. Moreover, the contamination occurred even at room

temperature, as shown in test No. 5 and Figure 8(i) and (j). A key lesson from tests No. 4 and 5 is that the nanocatalyzed MgH₂ system is very vulnerable to contaminant(s) and therefore must be well sealed in an impurity-free environment and protected during operation.

3.7. Temperature Oscillation Cycling (Nonisothermal Cycling). Previous cycling experiments are achieved by feeding hydrogen or evacuating for the samples. Another method to cycle the material is applying oscillating heating (thermal

cycling) to the sample. In this way, the sample is isolated in a closed volume throughout the cycling, while the temperature of hydride is periodically changed. Hydrogenation and dehydrogenation reactions can be realized at the lower-temperature period and higher-temperature period, respectively, due to shifting of the equilibrium pressure of MgH_2 . Details of this cycling experiment are given in experimental section 2.3.

The evolution of room-temperature hydrogenation with the cycling is plotted in Figure 9. The results show that a serious

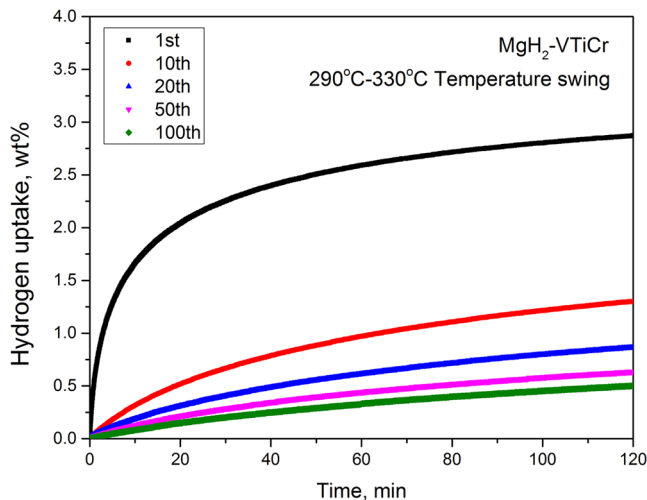


Figure 9. Hydrogenation kinetics after temperature-swing cycling of different cycles.

deterioration took place during the cycling. Because the sample chamber was always sealed without feeding hydrogen gas and evacuation, it should rule out the possibility of introducing contaminants to the sample. Therefore, the degradation happening here cannot be attributed to contamination or oxidization. Moreover, the other dubious factor, the high-temperature thermal annealing, is considered to be less important since the previous tests demonstrated that the sample (either in the Mg phase or in the MgH_2 phase) showed limited degradation on the kinetics after annealing with hydrogen pressure at 300 °C for 40 h. Consequently, it is suspected that the degradation was primarily due to the hydrogenation–dehydrogenation cycling.

3.8. Thermodynamics Properties Before and After Cycling. Thermodynamic properties of $\text{MgH}_2\text{-VTiCr}$ were characterized by using PCI measurement, and their PCI equilibrium curves at 300 °C were compared in Figure 10(a). First of all, the range of the plateau of the sample after 500 cycles indicates an available hydrogen capacity of 6.2 wt %, which is the same as that of the as-milled sample, demonstrating no loss of the hydrogen capacity after 500 cycles. The results also show that the equilibrium pressure of the cycled material remains essentially unchanged compared to that of the as-milled sample. Moreover, the van't Hoff plot of as-milled and as-cycled samples is provided in Figure 10(b). It was found that the cycled material had less hysteresis compared to the as-milled one.

4. DISCUSSION

From the results shown above, it was demonstrated that the catalyzed MgH_2 systems have a good stability at high temperatures (the temperature range of 300–400 °C).

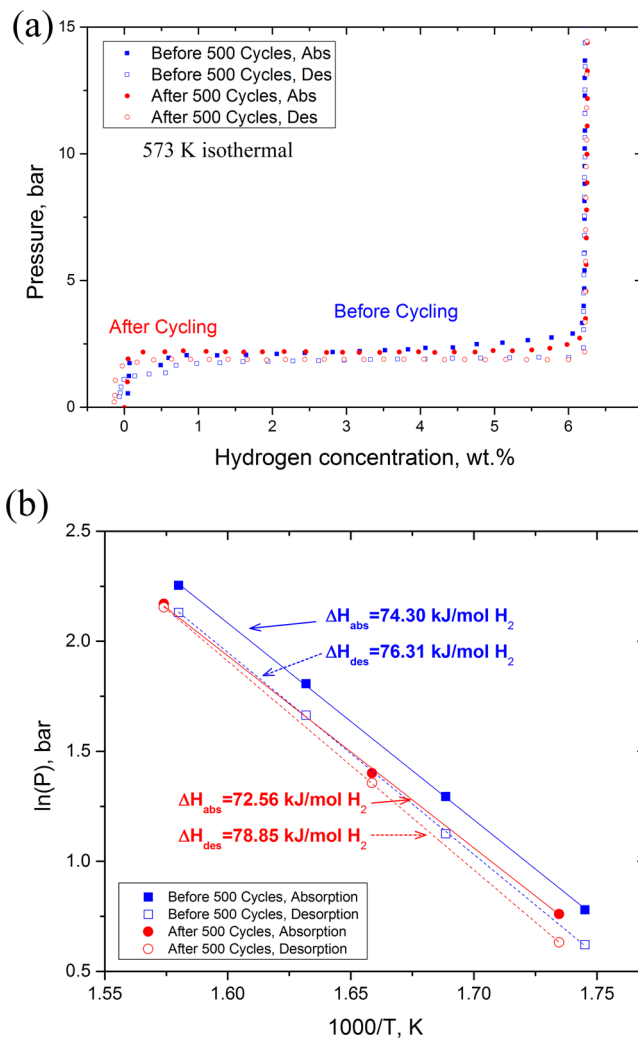


Figure 10. Thermodynamic properties of activated after as-milled $\text{MgH}_2\text{-VTiCr}$ (blue) and the same sample after 500 cycles (red). (a) Equilibrium pressure measurements performed at 300 °C. (b) Relative van't Hoff plot of the $\text{MgH}_2\text{-VTiCr}$ system before and after 500 cycles.

However, it is also realized that the hydrogenation kinetics of catalyzed MgH_2 at low temperature (the temperature range of 25–150 °C) suffered severe deterioration after cycling.

Using the well-established Johnson–Mehl–Avrami (JMA) model, we fit kinetic data of low-temperature hydrogenation to analyze the kinetic rate mathematically.^{45–47} The JMA model is described as

$$f = 1 - \exp(-kt)^n$$

where f is the transformed fraction; k is the kinetic rate constant; t is the reaction time; and n is the value of the Avrami exponent. Using the above equation, value of k can be calculated. As shown in Figure 11(a) and (b), the k of hydrogenation kinetics against cycle number were plotted. Figure 11(a) provides the relationship of k versus cycle number for the three different catalyst-doped systems (TiH_2 -catalyzed, TiMn_2 -catalyzed, and VTiCr -catalyzed MgH_2 , see original data in Figure 4). It can be seen that the behaviors of degradation for the three systems are similar. However, the $\text{MgH}_2\text{-VTiCr}$ system presents a higher resistance against extension of cycles. Figure 11(b) compares the relationship of k vs cycle number

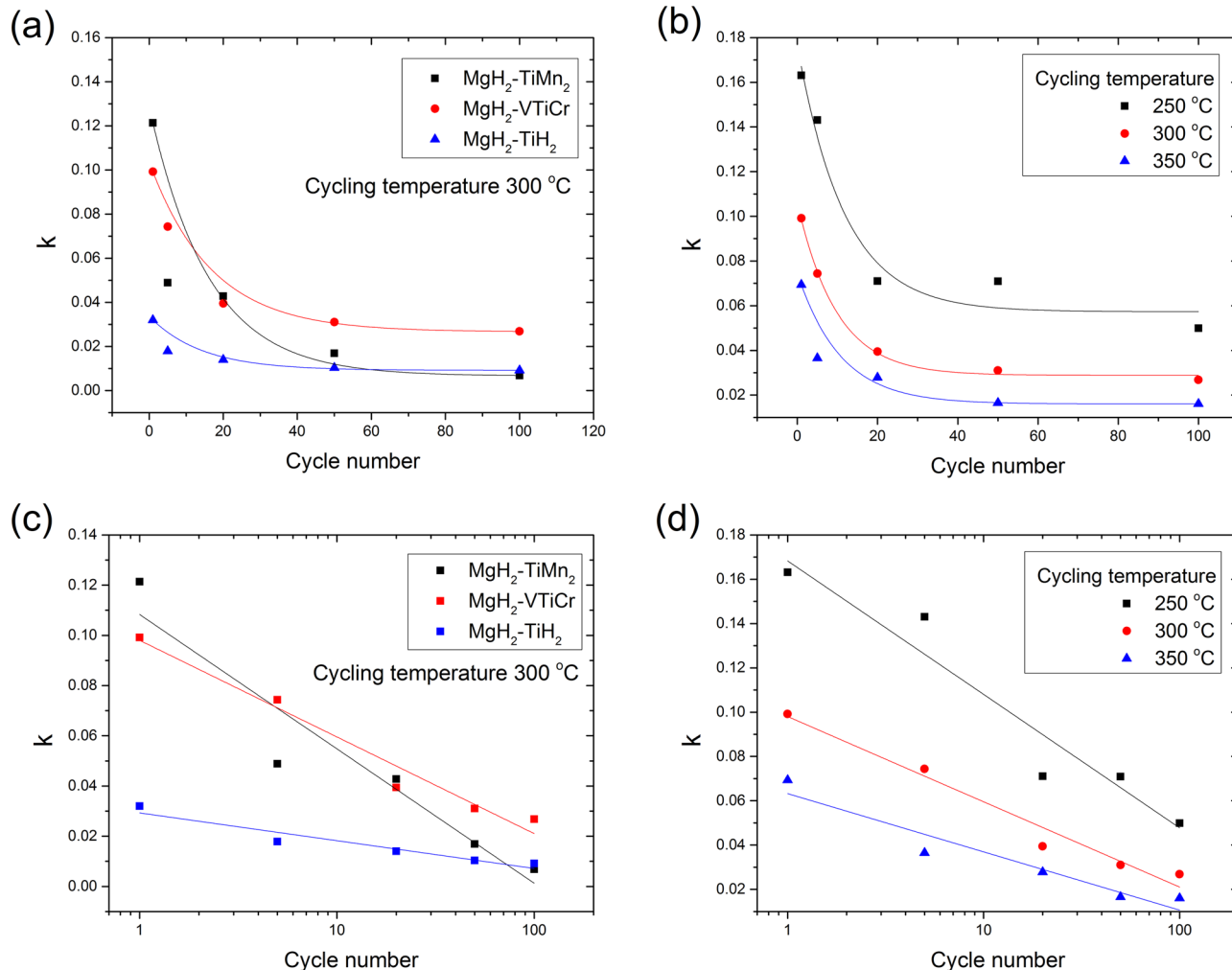


Figure 11. Plots of k versus cycle number. (a) k versus cycle number for TiH_2 -catalyzed, TiMn_2 -catalyzed, and VTiCr -catalyzed MgH_2 systems; (b) k versus cycle number cycling at 250, 300, and 350 °C; (c) and (d) are replotted (a) and (b) by using the logarithmic x axis.

for the cycling tests performed at different temperatures (see original data of kinetic curves in Figure 6). Furthermore, when the cycle numbers (value of x axis) in Figure 11(a) and (b) were logarithmically spaced, the k values and logarithm of cycle number present a relation of linear decay, as shown in Figure 11(c) and (d).

Generally, it is considered that the degradation is due to the following potential reasons:

- (1) Loss of hydrogen capacity
- (2) High-temperature thermal effect
- (3) Contamination
- (4) Reversed cycling reactions

It was observed that loss of hydrogen capacity occurred during the first 10 cycles of the cycling test. It is logical, therefore, to suggest that the unreacted hydride phase could impede the phase transformation at the next cycle. Comparing the cycling tests performed of different systems, the losses of hydrogen capacity after 100 cycles varied from 0.2 to 1.0 wt %. However, all the loss of hydrogen capacity took place during the first 10 cycles. Therefore, the presence of the unreacted hydride phase is probably one of the main reasons for the degradation of the low-temperature hydrogenation kinetics in the first 10 cycles.

As discussed in the result section 3.6, no significant degradation was found after annealing the sample at 300 °C for 40 h. Regardless the potential outcome of the high-temperature thermal effect such as reduction of surface area and grain growth of Mg/MgH_2 , the results indicates that the exposure to the elevated temperature (300 °C) is unlikely to be the main reason that leads to the degradation of room-temperature kinetics.

Contamination and/or oxidation is directly related to a kinetic degradation of not only the room-temperature hydrogenation but also the high-temperature dehydrogenation.⁴⁸ A common belief is that in the presence of O_2 or H_2O or other contaminants an oxide shell can form on the surface of Mg particles. The oxide (MgO) can block diffusion of hydrogen.^{49,50} For our cycling tests (both isothermal and non-isothermal cycling), severe oxidation to the materials should be ruled out because no loss of hydrogen capacity could be observed by plateau (PCI) measurements. It is expected that in our thermal annealing tests, when the evacuating process with the mechanical pump was actively vacuuming for 40 h, contaminant(s) may be introduced into the sample chamber, and oxide may accumulate on the surface of the material.

It has to be pointed out that the room-temperature hydrogenation kinetics exhibited significant degradation after temperature oscillation cycling. This cycling method had the

material sealed in the sample chamber throughout the cycling so there is no chance of introducing any contaminant. This fact indicates that a key factor that strongly affects the room-temperature hydrogenation kinetics is the reversed cycling reactions. As reported by Tan et al.,³⁹ the microstructure of the Mg–Nb–V system changed drastically after hydrogen cycling. In the accompanying paper, part II (<http://dx.doi.org/10.1021/acs.jpcc.5b06192>), characterization results and mechanistic discussion will be provided.

5. CONCLUSION

A comprehensive study of cyclic stability of catalyzed MgH₂ was conducted. Results show that both the hydrogenation and dehydrogenation kinetics at 300 °C were generally stable during 100 cycles. However, at the low temperatures (25–150 °C), the hydrogenation kinetics suffered a severe degradation after the cycling. Among the different catalyzed systems (TiH₂-catalyzed, TiMn₂-catalyzed, and VTiCr-catalyzed MgH₂), the MgH₂–VTiCr system exhibited better kinetics against hydrogen cycling. As elaborated in a companion paper (i.e., MgH₂ Cycling-II), the low-temperature kinetic degradation can be mainly attributed to microstructural grain growth during the extended hydrogenation–dehydrogenation reactions. Namely, the characterization of uncycled and cycled catalyzed MgH₂ by XRD, SEM, and TEM indicated the crystallite sizes of the Mg and MgH₂ significantly increased after the cycling as well as changes in the catalyst particles.

■ ASSOCIATED CONTENT

Supporting Information

The Supporting Information is available free of charge on the ACS Publications website at DOI: [10.1021/acs.jpcc.5b06190](http://dx.doi.org/10.1021/acs.jpcc.5b06190).

Detailed information of the nonisothermal cycling test (PDF)

■ AUTHOR INFORMATION

Corresponding Author

*E-mail: zak.fang@utah.edu.

Notes

The authors declare no competing financial interest.

■ ACKNOWLEDGMENTS

This research was supported by the U.S. Department of Energy (DOE) under contract number DE-AR0000173.

■ REFERENCES

- (1) Schlapbach, L.; Zuttel, A. Hydrogen-Storage Materials for Mobile Applications. *Nature* **2001**, *414*, 353–358.
- (2) Sakintuna, B.; Lamari-Darkrim, F.; Hirscher, M. Metal Hydride Materials for Solid Hydrogen Storage: A Review. *Int. J. Hydrogen Energy* **2007**, *32*, 1121–1140.
- (3) Jain, I. P.; Lal, C.; Jain, A. Hydrogen Storage in Mg: A Most Promising Material. *Int. J. Hydrogen Energy* **2010**, *35*, 5133–5144.
- (4) Huot, J.; Ravnsbæk, D. B.; Zhang, J.; Cuevas, F.; Latroche, M.; Jensen, T. R. Mechanochemical Synthesis of Hydrogen Storage Materials. *Prog. Mater. Sci.* **2013**, *58*, 30–75.
- (5) Harries, D. N.; Paskevicius, M.; Sheppard, D. A.; Price, T. E. C.; Buckley, C. E. Concentrating Solar Thermal Heat Storage Using Metal Hydrides. *Proc. IEEE* **2012**, *100*, 539–549.
- (6) Fang, Z. Z.; Zhou, C.; Fan, P.; Udell, K. S.; Bowman, R. C.; Vajo, J. J.; Purewal, J. J.; Kekelia, B. Metal Hydrides Based High Energy Density Thermal Battery. *J. Alloys Compd.* **2015**, *645*, S184.
- (7) Bogdanović, B.; Ritter, A.; Spiethoff, B. Active MgH₂-Mg Systems for Reversible Chemical Energy Storage. *Angew. Chem., Int. Ed. Engl.* **1990**, *29*, 223–234.
- (8) Wierse, M.; Werner, R.; Groll, M. Magnesium Hydride for Thermal Energy Storage in a Small-Scale Solar-Thermal Power Station. *J. Less-Common Met.* **1991**, *172*–*174*, 1111–1121.
- (9) Reiser, A.; Bogdanović, B.; Schlichte, K. The Application of Mg-Based Metal-Hydrides as Heat Energy Storage Systems. *Int. J. Hydrogen Energy* **2000**, *25*, 425–430.
- (10) Rönnebro, E. C. E.; Majzoub, E. H. Recent Advances in Metal Hydrides for Clean Energy Applications. *MRS Bull.* **2013**, *38*, 452–458.
- (11) Delhomme, B.; de Rango, P.; Marty, P.; Bacia, M.; Zawilski, B.; Raufast, C.; Miraglia, S.; Fruchart, D. Large Scale Magnesium Hydride Tank Coupled with an External Heat Source. *Int. J. Hydrogen Energy* **2012**, *37*, 9103–9111.
- (12) Zhou, C.; Fang, Z. Z.; Lu, J.; Luo, X.; Ren, C.; Fan, P.; Ren, Y.; Zhang, X. Thermodynamic Destabilization of Magnesium Hydride Using Mg-Based Solid Solution Alloys. *J. Phys. Chem. C* **2014**, *118*, 11526–11535.
- (13) Liang, G.; Huot, J.; Boily, S.; Van Neste, A.; Schulz, R. Hydrogen Storage Properties of the Mechanically Milled MgH₂-V Nanocomposite. *J. Alloys Compd.* **1999**, *291*, 295–299.
- (14) Choi, Y. J.; Lu, J.; Sohn, H. Y.; Fang, Z. Z. Hydrogen Storage Properties of the Mg-Ti-H System Prepared by High-Energy-High-Pressure Reactive Milling. *J. Power Sources* **2008**, *180*, 491–497.
- (15) Choi, Y. J.; Lu, J.; Sohn, H. Y.; Fang, Z. Z.; Rönnebro, E. Effect of Milling Parameters on the Dehydrogenation Properties of the Mg–Ti–H System. *J. Phys. Chem. C* **2009**, *113*, 19344–19350.
- (16) Liang, G.; Huot, J.; Boily, S.; Van Neste, A.; Schulz, R. Catalytic Effect of Transition Metals on Hydrogen Sorption in Nanocrystalline Ball Milled MgH₂–Tm (Tm = Ti, V, Mn, Fe and Ni) Systems. *J. Alloys Compd.* **1999**, *292*, 247–252.
- (17) House, S. D.; Vajo, J. J.; Ren, C.; Rockett, A. A.; Robertson, I. M. Effect of Ball-Milling Duration and Dehydrogenation on the Morphology, Microstructure and Catalyst Dispersion in Ni-Catalyzed MgH₂ Hydrogen Storage Materials. *Acta Mater.* **2015**, *86*, 55–68.
- (18) Niessen, R. A. H.; Notten, P. H. L. Electrochemical Hydrogen Storage Characteristics of Thin Film MgX (X = Sc, Ti, V, Cr) Compounds. *Electrochim. Solid-State Lett.* **2005**, *8*, A534–A538.
- (19) Kalisvaart, W. P.; Kubis, A.; Danaie, M.; Amirkhiz, B. S.; Mitlin, D. Microstructural Evolution During Hydrogen Sorption Cycling of Mg–FeTi Nanolayered Composites. *Acta Mater.* **2011**, *59*, 2083–2095.
- (20) Zheng, S.; Wang, K.; Oleshko, V. P.; Bendersky, L. A. Mg–Fe Thin Films: A Phase-Separated Structure with Fast Kinetics of Hydrogenation. *J. Phys. Chem. C* **2012**, *116*, 21277–21284.
- (21) Mooij, L. P. A.; Baldi, A.; Boelsma, C.; Shen, K.; Wagemaker, M.; Pivak, Y.; Schreuders, H.; Griessen, R.; Dam, B. Interface Energy Controlled Thermodynamics of Nanoscale Metal Hydrides. *Adv. Energy Mater.* **2011**, *1*, 754–758.
- (22) Schimmel, H. G.; Huot, J.; Chapon, L. C.; Tichelaar, F. D.; Mulder, F. M. Hydrogen Cycling of Niobium and Vanadium Catalyzed Nanostructured Magnesium. *J. Am. Chem. Soc.* **2005**, *127*, 14348–14354.
- (23) Pelletier, J. F.; Huot, J.; Sutton, M.; Schulz, R.; Sandy, A. R.; Lurio, L. B.; Mochrie, S. G. J. Hydrogen Desorption Mechanism in MgH₂-Nb Nanocomposites. *Phys. Rev. B: Condens. Matter Mater. Phys.* **2001**, *63*, 052103.
- (24) Friedrichs, O.; Aguey-Zinsou, F.; Fernández, J. R. A.; Sánchez-López, J. C.; Justo, A.; Klassen, T.; Bormann, R.; Fernández, A. MgH₂ with Nb₂O₅ as Additive, for Hydrogen Storage: Chemical, Structural and Kinetic Behavior with Heating. *Acta Mater.* **2006**, *54*, 105–110.
- (25) Friedrichs, O.; Klassen, T.; Sánchez-López, J. C.; Bormann, R.; Fernández, A. Hydrogen Sorption Improvement of Nanocrystalline MgH₂ by Nb₂O₅ Nanoparticles. *Scr. Mater.* **2006**, *54*, 1293–1297.
- (26) Hanada, N.; Ichikawa, T.; Fujii, H. Hydrogen Absorption Kinetics of the Catalyzed MgH₂ by Niobium Oxide. *J. Alloys Compd.* **2007**, *446*–*447*, 67–71.

- (27) Lu, J.; Choi, Y. J.; Fang, Z. Z.; Sohn, H. Y.; Rönnebro, E. Hydrogen Storage Properties of Nanosized $MgH_2\text{-}0.1TiH_2$ Prepared by Ultrahigh-Energy-High-Pressure Milling. *J. Am. Chem. Soc.* **2009**, *131*, 15843–15852.
- (28) Lu, J.; Choi, Y. J.; Fang, Z. Z.; Sohn, H. Y.; Rönnebro, E. Hydrogenation of Nanocrystalline Mg at Room Temperature in the Presence of TiH_2 . *J. Am. Chem. Soc.* **2010**, *132*, 6616–6617.
- (29) Zahiri, B.; Danaie, M.; Tan, X.; Amirkhiz, B. S.; Botton, G. A.; Mitlin, D. Stable Hydrogen Storage Cycling in Magnesium Hydride, in the Range of Room Temperature to 300 °C, Achieved Using a New Bimetallic Cr-V Nanoscale Catalyst. *J. Phys. Chem. C* **2011**, *116*, 3188–3199.
- (30) Zahiri, B.; Amirkhiz, B. S.; Mitlin, D. Hydrogen Storage Cycling of MgH_2 Thin Film Nanocomposites Catalyzed by Bimetallic Cr-Ti. *Appl. Phys. Lett.* **2010**, *97*, 083106–3.
- (31) Zahiri, B.; Amirkhiz, B. S.; Danaie, M.; Mitlin, D. Bimetallic Fe-V Catalyzed Magnesium Films Exhibiting Rapid and Cycleable Hydrogenation at 200 °C. *Appl. Phys. Lett.* **2010**, *96*, 013108–3.
- (32) Zahiri, B.; Harrower, C. T.; Amirkhiz, B. S.; Mitlin, D. Rapid and Reversible Hydrogen Sorption in Mg-Fe-Ti Thin Films. *Appl. Phys. Lett.* **2009**, *95*, 103114–3.
- (33) Zhou, C.; Fang, Z. Z.; Lu, J.; Zhang, X. Thermodynamic and Kinetic Destabilization of Magnesium Hydride Using Mg-In Solid Solution Alloys. *J. Am. Chem. Soc.* **2013**, *135*, 10982–10985.
- (34) Zhou, C.; Fang, Z. Z.; Ren, C.; Li, J.; Lu, J. Effect of Ti Intermetallic Catalysts on Hydrogen Storage Properties of Magnesium Hydride. *J. Phys. Chem. C* **2013**, *117*, 12973–12980.
- (35) Ren, C.; Fang, Z. Z.; Zhou, C.; Lu, J.; Ren, Y.; Zhang, X. Hydrogen Storage Properties of Magnesium Hydride with V-Based Additives. *J. Phys. Chem. C* **2014**, *118*, 21778–21784.
- (36) Zhou, C.; Fang, Z. Z.; Sun, P. An Experimental Survey of Additives for Improving Dehydrogenation Properties of Magnesium Hydride. *J. Power Sources* **2015**, *278*, 38–42.
- (37) Dehouche, Z.; Klassen, T.; Oelerich, W.; Goyette, J.; Bose, T. K.; Schulz, R. Cycling and Thermal Stability of Nanostructured $MgH_2\text{-}Cr_2O_3$ Composite for Hydrogen Storage. *J. Alloys Compd.* **2002**, *347*, 319–323.
- (38) Dehouche, Z.; Djaozandry, R.; Huot, J.; Boily, S.; Goyette, J.; Bose, T. K.; Schulz, R. Influence of Cycling on the Thermodynamic and Structure Properties of Nanocrystalline Magnesium Based Hydride. *J. Alloys Compd.* **2000**, *305*, 264–271.
- (39) Tan, X.; Zahiri, B.; Holt, C. M. B.; Kubis, A.; Mitlin, D. A TEM Based Study of the Microstructure During Room Temperature and Low Temperature Hydrogen Storage Cycling in MgH_2 Promoted by Nb–V. *Acta Mater.* **2012**, *60*, 5646–5661.
- (40) Amirkhiz, B. S.; Zahiri, B.; Kalisvaart, P.; Mitlin, D. Synergy of Elemental Fe and Ti Promoting Low Temperature Hydrogen Sorption Cycling of Magnesium. *Int. J. Hydrogen Energy* **2011**, *36*, 6711–6722.
- (41) Kalisvaart, W. P.; Harrower, C. T.; Haagsma, J.; Zahiri, B.; Luber, E. J.; Ophus, C.; Poirier, E.; Fritzsche, H.; Mitlin, D. Hydrogen Storage in Binary and Ternary Mg-Based Alloys: A Comprehensive Experimental Study. *Int. J. Hydrogen Energy* **2010**, *35*, 2091–2103.
- (42) Zahiri, R.; Zahiri, B.; Kubis, A.; Kalisvaart, P.; Shalchi Amirkhiz, B.; Mitlin, D. Microstructural Evolution During Low Temperature Sorption Cycling of Mg-AlTi Multilayer Nanocomposites. *Int. J. Hydrogen Energy* **2012**, *37*, 4215–4226.
- (43) Bowman, R. C., Jr; Luo, C. H.; Ahn, C. C.; Witham, C. K.; Fultz, B. The Effect of Tin on the Degradation of $LaNi_{5-y}Sn_y$ Metal Hydrides During Thermal Cycling. *J. Alloys Compd.* **1995**, *217*, 185–192.
- (44) Dehouche, Z.; Goyette, J.; Bose, T. K.; Schulz, R. Moisture Effect on Hydrogen Storage Properties of Nanostructured $MgH_2\text{-}V\text{-}Ti$ Composite. *Int. J. Hydrogen Energy* **2003**, *28*, 983–988.
- (45) Sabitu, S. T.; Fagbami, O.; Goudy, A. J. Kinetics and Modeling Study of Magnesium Hydride with Various Additives at Constant Pressure Thermodynamic Driving Forces. *J. Alloys Compd.* **2011**, *509*, S588–S591.
- (46) Li, J.; Fan, P.; Fang, Z. Z.; Zhou, C. Kinetics of Isothermal Hydrogenation of Magnesium with TiH_2 Additive. *Int. J. Hydrogen Energy* **2014**, *39*, 7373–7381.
- (47) Mooij, L.; Dam, B. Nucleation and Growth Mechanisms of Nano Magnesium Hydride from the Hydrogen Sorption Kinetics. *Phys. Chem. Chem. Phys.* **2013**, *15*, 11501–11510.
- (48) Bouaricha, S.; Huot, J.; Guay, D.; Schulz, R. Reactivity During Cycling of Nanocrystalline Mg-based Hydrogen Storage Compounds. *Int. J. Hydrogen Energy* **2002**, *27*, 909–913.
- (49) Friedrichs, O.; Sánchez-López, J. C.; López-Cartes, C.; Dornheim, M.; Klassen, T.; Bormann, R.; Fernández, A. Chemical and Microstructural Study of the Oxygen Passivation Behaviour of Nanocrystalline Mg and MgH_2 . *Appl. Surf. Sci.* **2006**, *252*, 2334–2345.
- (50) Ostenfeld, C. W.; Chorkendorff, I. Effect of Oxygen on the Hydrogenation Properties of Magnesium Films. *Surf. Sci.* **2006**, *600*, 1363–1368.